Appendix A GPS Analysis

The hypothesis of episodic slow slip has been postulated by employing solely horizontal GPS recordings. Here, we use all three components of GPS recording (two horizontal and one vertical) to demonstrate the 3D deformation of the continental crust over time and how their magnitudes relate to tremor location.

A1 Reliability of Vertical GPS Measurements

Uncertainty in vertical GPS measurements is approximately 3 times that of horizontal measurements. More importantly, we recognize that seasonal variations in surface mass variations can have substantial impact on vertical GPS measurements Blewitt et al. (2001); Dong et al. (2002); Bettinelli et al. (2008).

Here, however, we ignore the effect of seasonal changes on vertical GPS measurements because it is extremely challenging to decouple the effect of seasonal surficial mass changes from displacement due to tectonic deformation. This task become especially challenging in Cascadia where the episodic deformation cycle spans 13–14 months which is close to seasonal cycles (12 months).

Nonetheless, we observe that

- vertical GPS measurements are large and in many cases an order of magnitude larger than horizontal displacements,
- there is a close correspondence between sudden changes in horizontal displacements (horizontal GPS reversals) and rapid vertical GPS measurements on numerous occasions, and
- vertical cyclic displacement patterns (Figure A3 and A4) show close spatial correspondence with spatial tremor patterns in Cascadia and Alaska.

Given the above observations, one might argue that vertical displacements observed contain significant imprints of tectonic deformation.

A2 Data Processing

Prior to hodogram analysis, GPS data are detrended using a 1001 point median filter to eliminate long-term trends, and thereafter filtered using a 11-point median filter to suppress short-term noise bursts. GPS stations with significant noise that could not be corrected from using the above filtering operations were not used in the analysis.

Computation of the net vertical and horizontal GPS displacements was done by fitting ellipsoids to the hodograms. Projection of the major axis of the ellipse on the vertical direction and the horizontal plane yield the net vertical and horizontal displacements, respectively.

A3 Displacements due to Buckling and Collapse

Figure A1 shows the expected temporal evolution of the vertical (blue) and horizontal (red) displacements of four locations A, B, C, and D, (phase T_0, Figure 2) on the surface of a continental plate through a buckling and collapsing cycle. The magnitude of the horizontal displacement is expected to decrease monotonically from the corner of the accretionary wedge (location A) landward as depicted by the decreasing range of the horizontal displacement moving from A through D. The vertical displacement, however, is small at location A, attains a maximum at location C, and tapers off to a small value further landwards (location D).

An efficient technique to analyze and quantify such multi-component data is to generate hodograms which are a display of the motion of a point as a function of time. Figure A1 shows the hodograms for each of the four locations A, B, C, and D on the right. The path followed by a particle during the buckling phase is different from that followed during the collapse phase, thereby resulting in hysteresis of the particle motion. Note that such hysteresis demonstrates a non-linear particle motion (Figure A1) as opposed to an expected linear motion for the case of slow slip. Moreover, it is clear from the hodograms that the horizontal displacement decreases monotonically from the corner of the accretionary wedge (location A) landward, while the vertical displacement attains a maximum right above the narrow tremor zone.

Figure A2 shows an example of a hodogram obtained from GPS data. This data comes from the Albert Head GPS site on Vancouver Island in Victoria, British Columbia – the data for which was originally employed by Rogers and Dragert (2003) to hypothesize the process of slow slip. Note the hysteresis and the prominent vertical displacement observed at this site which is quite similar to the pattern expected for surface location C (Figure A1) right above a tremor belt. Other studies (Wech et al., 2009; Wells et al., 2017) indeed map significant tremor activity beneath this GPS site.

A4 Horizontal and Vertical Displacements in Cascadia and Alaska

We generate hodograms for all the GPS measurements at sites in the Cascadia subduction zone and in Alaska and thereafter compute the vertical displacement, horizontal displacement, and their ratio. These attributes for Cascadia and Alaska are shown in Figures A3 and A4, respectively. Note that in both cases, the horizontal displacement decreases monotonically from the margin landwards; while the vertical displacement increases as one moves landwards from the margin, attains a maximum, and decreases thereafter. The belt of maximum vertical displacements along the Cascadia margin has a close correspondence to the tremor maps generated by Wech et al. (2009); Wells et al. (2017). Similarly, the maximum vertical displacements in Alaska encompass the tremor activity mapped by Y. Ohta et al. (2006) and Peterson and Christensen (2009) (in addition to showing locations where additional tremor activity could be expected).

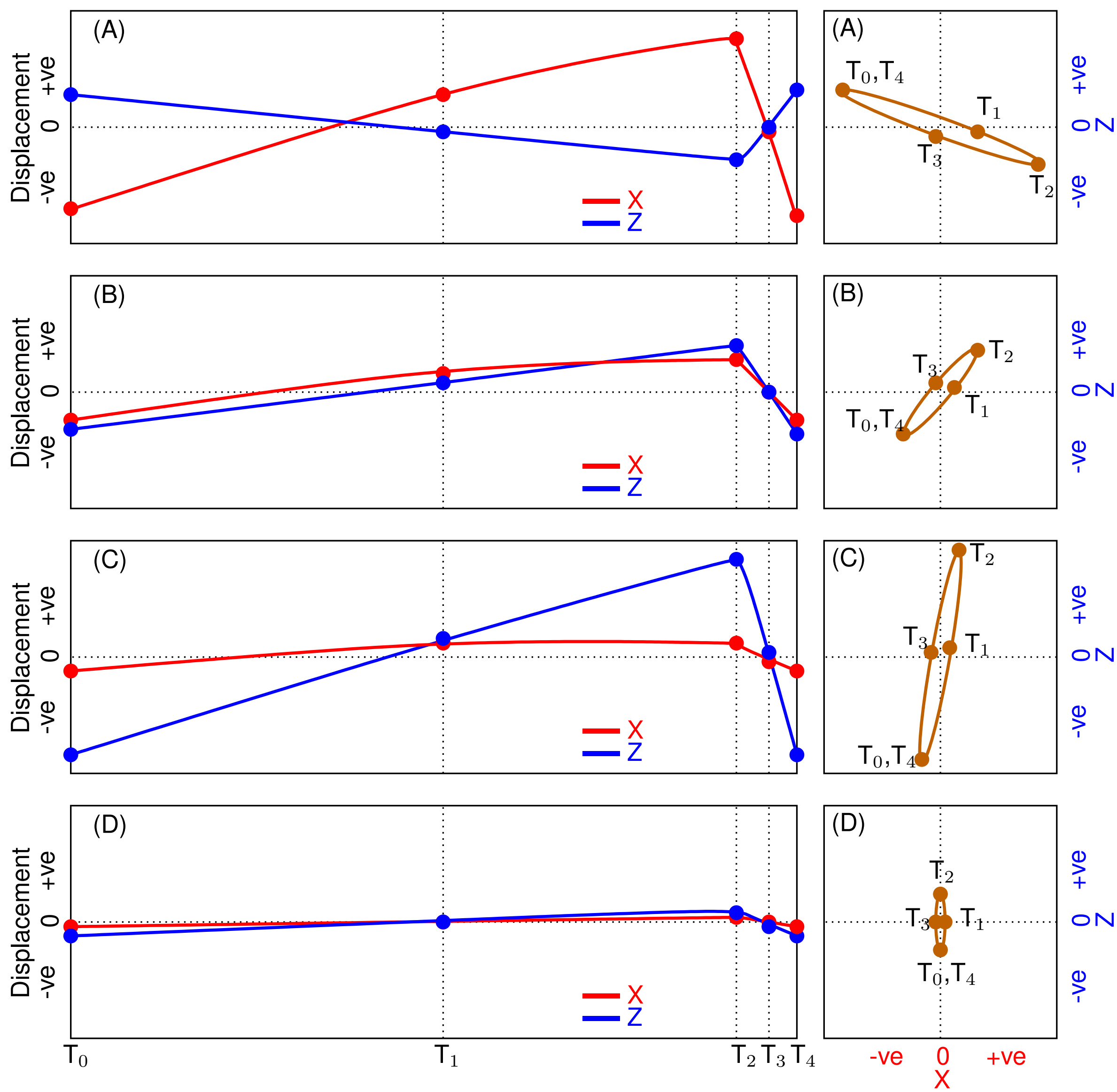

Figure A1: **Time-dependent detrended displacements (left column) and corresponding hodograms (right column) of points A through D (Figure2) during a single cycle of Episodic Buckling and Collapse.** Horizontal displacement X is shown in red and vertical displacement Z in blue. The different phases of the subduction cycle are also denoted.

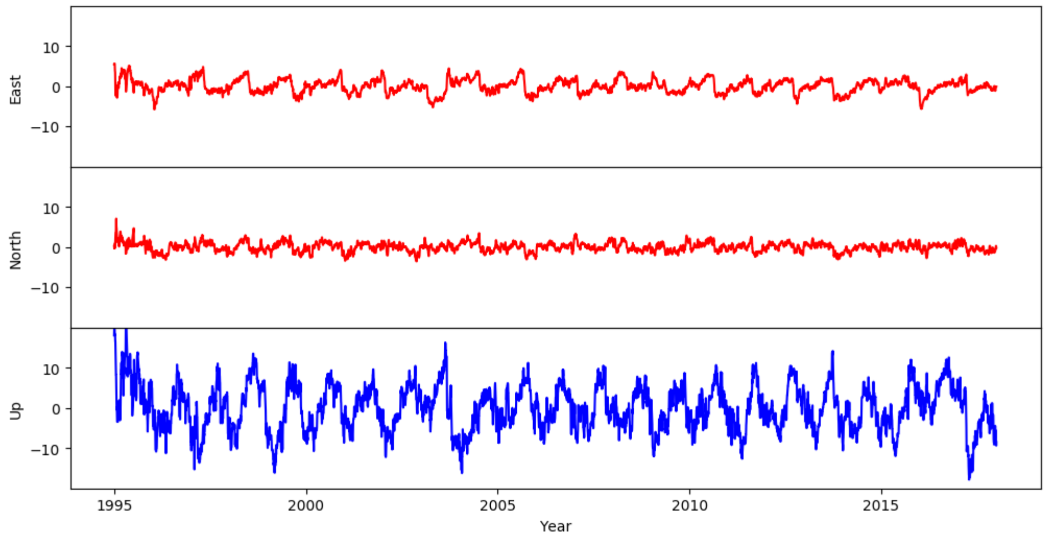

(a) GPS

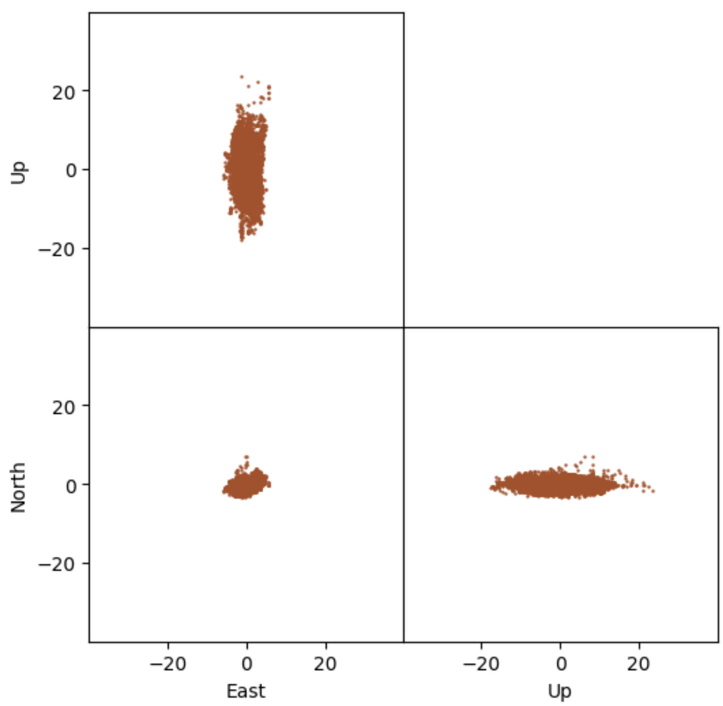

(b) Hodogram

Figure A2: **East, North, and vertical components of GPS data and corresponding hodogram from the Albert Head GPS site on Vancouver Island in Victoria, British Columbia and corresponding hodogram on the right.** All data have been detrended and filtered. The hodogram is displayed in the form of projections on the three orthogonal planes.

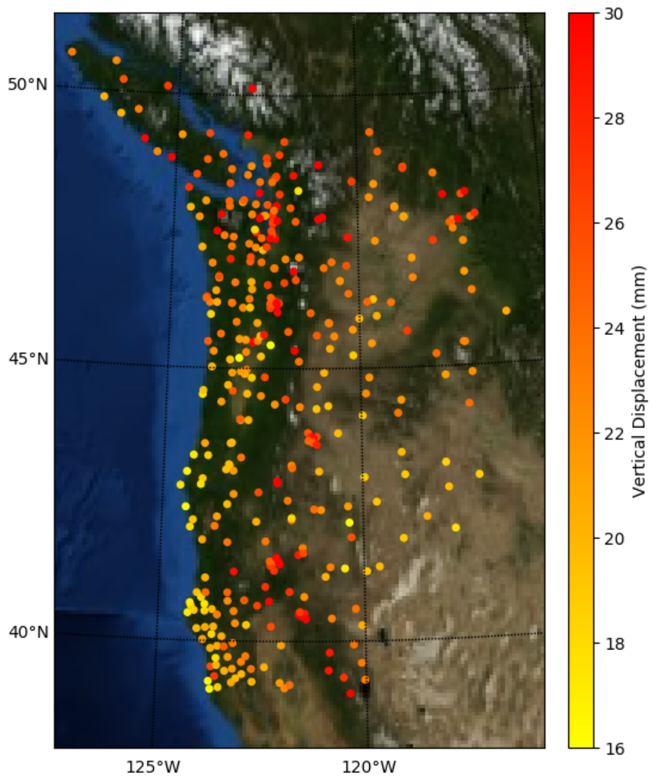

(a) Vertical displacement

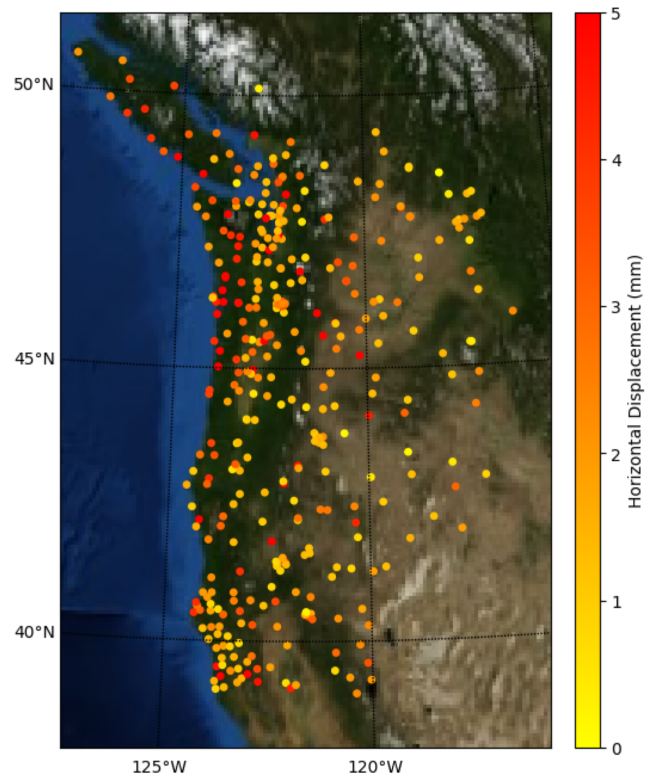

(b) Horizontal displacement

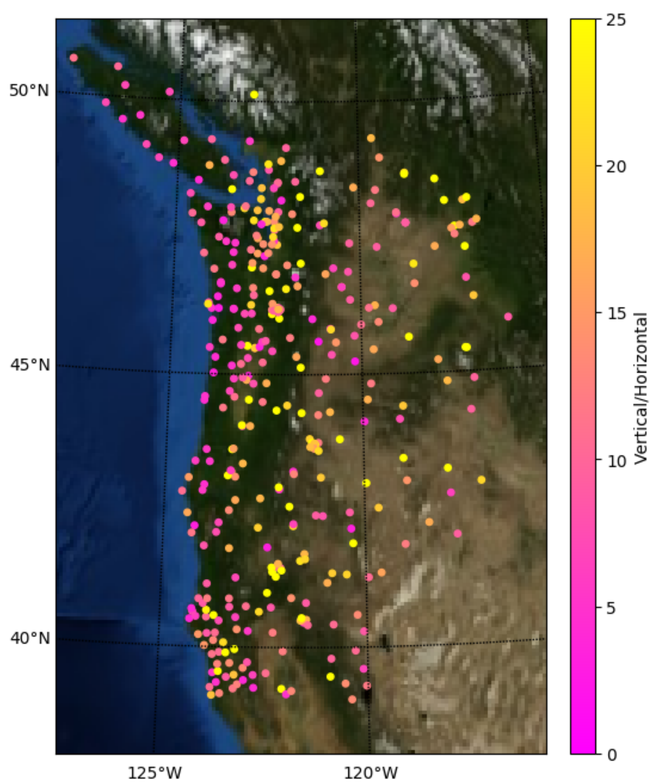

(c) Vertical-Horizontal Ratio

Figure A3: **Measures of surface deformation in Cascadia subduction zone. a,** Net vertical displacement and **b,** net horizontal displacement computed from GPS measurements, and **c,** their ratio. All color scales have been truncated to expose the patterns.

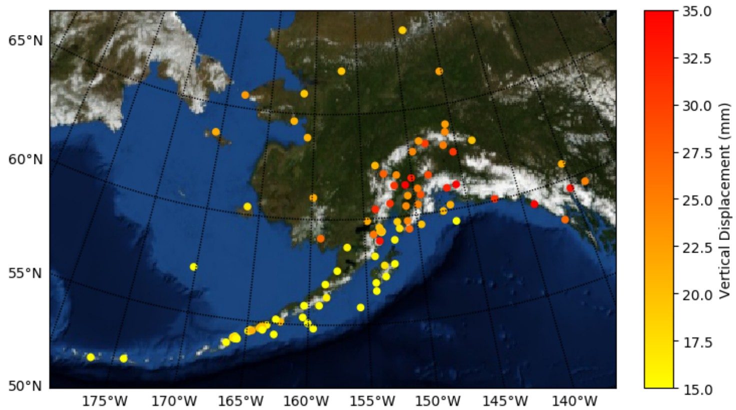

(a) Vertical displacement

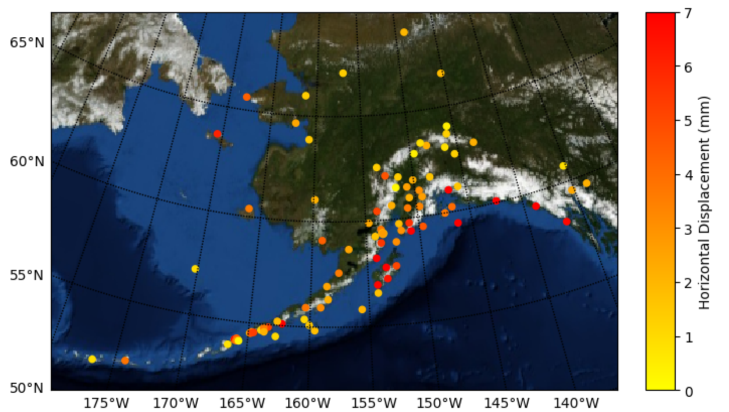

(b) Horizontal displacement

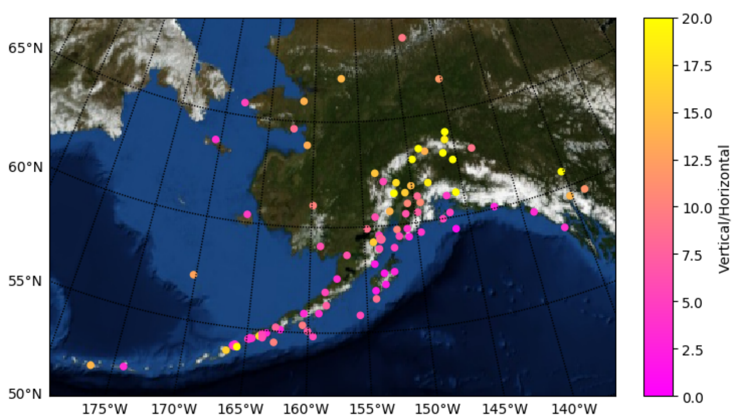

(c) Vertical-Horizontal Ratio

Figure A4: **Measures of surface deformation in Alaska. a,** Net vertical displacement and **b,** net horizontal displacement computed from GPS measurements, and **c,** their ratio. All color scales have been truncated to expose the patterns.